Integration of Antiangiogenic Therapy with Cisplatin and Gemcitabine Chemotherapy in Patients with Nasopharyngeal Carcinoma

Wan Qin Chong[1], Chwee Ming Lim[2], Arvind Kumar Sinha[3], Chee Seng Tan[1], Gloria Hui Jia Chan[1], Yiqing Huang[1], Nesaretnam Barr Kumarakulasinghe[1], Raghav Sundar[1], Anand D. Jeyasekharan[1,4], Woei Shyang Loh[2], Joshua K. Tay[2], Kritika Yadav[4], Lingzhi Wang[4,5], Andrea L. Wong[1,4], Li Ren Kong[4], Ross Andrew Soo[1,4], Jieying Amelia Lau[4], Yu Yang Soon[6], Robby Miguel Goh[1], Francis Cho Hao Ho[6], Siew Meng Chong[7,†], Soo Chin Lee[1,4], Kwok Seng Loh[2], Bee Choo Tai[8], Yaw Chyn Lim[7,9,*], and Boon Cher Goh[1,4,5,*]

ABSTRACT

Purpose: Induction cisplatin and gemcitabine chemotherapy is a standard treatment for locally advanced nasopharyngeal carcinoma (NPC). Inhibition of VEGF axis has been shown to promote maturation of microvasculature and improve perfusion. We conducted a four-arm study to assess the effect of two doses of either sunitinib or bevacizumab with chemotherapy in NPC.

Patients and Methods: Patients with treatment-naïve locally advanced NPC were treated with three cycles of 3-weekly cisplatin and gemcitabine preceded by 1 week of anti-VEGF therapy for each cycle, followed by standard concurrent chemoradiation: arm A patients received 7 days of 12.5 mg/day sunitinib; arm B 7 days of 25 mg/day sunitinib; arm C bevacizumab 7.5 mg/kg infusion; arm D bevacizumab 2.5 mg/kg infusion. Patients with metastatic NPC were treated with up to six cycles of similar treatment without concurrent chemoradiation.

Results: Complete metabolic response (mCR) by whole body ^{18}FDG PET was highest in arm C (significant difference in four groups Fisher exact test $P = 0.001$; type 1 error $= 0.05$), with 42% mCR (95% confidence interval, 18–67) and 3-year relapse-free survival of 88% in patients with locally advanced NPC. Significant increase in pericyte coverage signifying microvascular maturation and increased immune cell infiltration was observed in posttreatment tumor biopsies in Arm C. Myelosuppression was more profound in sunitinib containing arms, and tolerability was established in arm C where hypertension was the most significant toxicity.

Conclusions: Bevacizumab 7.5 mg/kg with cisplatin and gemcitabine was well tolerated. Promising tumor response was observed and supported mechanistically by positive effects on tumor perfusion and immune cell trafficking into the tumor.

Introduction

Nasopharyngeal cancer usually presents as locally advanced stage III or IV disease with T3-4 or N2-3 nodal status (1). The standard of care of patients with locally advanced nasopharyngeal carcinoma is concurrent cisplatin chemotherapy with radiotherapy (2). However, locally advanced stage IV patients with T4 or N3 disease have the highest risk of recurrence and metastasis; and may benefit from additional strategies to improve their outcome (3, 4). Emerging evidence suggests that induction chemotherapy improves patient survival in this group of patients when integrated with concurrent chemoradiation (5, 6). A meta-analysis also showed that the addition of induction chemotherapy improved overall survival, and reduced locoregional and distant failure (7).

Dysregulation of the VEGF/VEGF receptor-2 axis is a feature of many cancers including NPC. Elevated VEGF expression promotes disorganized tumor neovascularization with hyperpermeable, tortuous capillaries that have immature pericyte coverage (8, 9). Leakiness of vessels increases interstitial fluid pressure that collapses vessels with the collective effect of compromising blood flow and perfusion, limiting the delivery of therapeutic drugs. Furthermore, tumor expression of VEGF promotes immune tolerance directly and through hypoxic mechanisms, suppressing dendritic cell maturation, dampening immune activation through immunosuppressive cells like regulatory T cells, myeloid-derived suppressor cells, and M2 macrophage polarization (10). Recent meta-analysis has shown that high expression of VEGF in NPC was associated with inferior survival, and higher plasma levels of VEGF confounds the overall survival of patients (11). The VEGF/VEGFR-2 axis can be inhibited by small-molecule inhibitors like sunitinib, which target VEGFR 1–3, PDGFRα/β, stem cell factor receptor, Flt3, or with the humanized mAb bevacizumab, which

[1]Department of Haematology-Oncology, National University Cancer Institute, Singapore. [2]Department of Otolaryngology – Head and Neck Surgery, National University of Singapore, Singapore. [3]Department of Diagnostic Imaging, National University Health System, Singapore. [4]Cancer Science Institute of Singapore, NUS, Singapore. [5]Department of Pharmacology, National University of Singapore, Singapore. [6]Department of Radiation Oncology, National University Cancer Institute, Singapore. [7]Department of Pathology, National University of Singapore, Singapore. [8]School of Public Health, National University of Singapore, Singapore. [9]Department of Physiology, National University of Singapore, Singapore.

Note: Supplementary data for this article are available at Clinical Cancer Research Online (http://clincancerres.aacrjournals.org/).

Clinicaltrials.gov Registration ID: NCT01309633.

†Deceased.

*Y.C. Lim and B.C. Goh are co-corresponding authors.

Corresponding Author: Boon Cher Goh, National University Health System, 7th floor, NUHS Tower Block, 1E Lower Kent Road, Singapore 119228, Singapore. Phone: 656-772-4617; Fax: 0116567775545; E-mail: phcgbc@nus.edu.sg

Clin Cancer Res 2020;26:5320–8

doi: 10.1158/1078-0432.CCR-20-1727

Translational Relevance

Nasopharyngeal carcinoma often expresses high levels of VEGF which associates with poor clinical outcome in many studies. VEGF promotes disorganized tumor microvasculature, impairs drug delivery, and also promotes tumor immune tolerance by impairment of immune cell infiltration and suppression of mature dendritic cell function. In this four-arm study of anti-VEGF therapy combined with chemotherapy, bevacizumab was found to be better tolerated than sunitinib. Anti-VEGF therapy is able to effect maturation of tumor microvasculature, and improve immune cell infiltration in a dose-dependent way, with the best effect observed with bevacizumab at 7.5 mg/kg given 3-weekly. Bevacizumab at 7.5 mg/kg with cisplatin and gemcitabine showed high metabolic complete responses, leading to favorable relapse-free survival in locally advanced NPC. With the mechanistic understanding of anti-VEGF therapy in NPC, we recommend bevacizumab in combination with chemotherapy for further evaluation.

binds to VEGF-A and prevents ligand-receptor engagement. These inhibitors have the potential to modulate the tumor microenvironment positively through maturation of tumor microvasculature thus alleviating hypoxia and enhancing chemotherapy delivery and immune cell trafficking of anticancer activated T cells.

To test the hypothesis that addition of anti-VEGF therapy to chemotherapy is tolerable and active in NPC, we conducted a phase II open-label study using two doses of two different antiangiogenic therapies consisting of either sunitinib or bevacizumab in combination with cisplatin and gemcitabine chemotherapy as systemic therapy in patients with previously untreated locally advanced or metastatic NPC (Supplementary Fig. S1). As full doses of antiangiogenic treatment may excessively trim blood vessels leading to collapse of vasculature that compromises drug delivery, lower doses were initiated 7 days prior to chemotherapy to exploit the vascular normalization window of 3–8 days after VEGF inhibition as demonstrated in a glioblastoma model (12). Metabolic response was used as the primary endpoint of tumor efficacy for several reasons: in locally advanced NPC, nonfunctional imaging may lead to difficulty in interpreting tumor response due to overlap with normal structures, and prior studies have shown that PET CT responses have been associated with clinical outcome (13). Correlative studies of serial tumor biopsies were performed to evaluate the pharmacodynamic effects of VEGF inhibition in the tumor microenvironment prior to chemotherapy.

Patients and Methods

Patient selection

Eligible patients were at least 21 years old with American Joint Committee on Cancer 2010 stage III–IVC previously untreated histologically confirmed EBV-encoded RNA (EBER)-positive WHO type II or III NPC; Eastern Cooperative Oncology Group performance status of 0 or 1; adequate bone marrow, renal, and hepatic functions; and evaluable disease as per RECIST (version 1.1). Patients were excluded if they had uncontrolled hypertension, New York Heart Association grade ≥2 congestive heart failure, active coronary artery disease, arterial or venous thromboembolic events in the last 6 months, clinically significant bleeding in the last 30 days, or persistent proteinuria > 3.5 g/24 hours. Written informed consent was obtained before any study-related procedures, and the study protocol was approved by the ethics committee of the institution and was conducted in compliance with ethical guidelines in the Declaration of Helsinki. (Clinicaltrials.gov ID: NCT01309633).

Study design and treatment

This was an open-label, phase II trial of cisplatin and gemcitabine with four cohorts: two doses of sunitinib (arm A and B) and bevacizumab (arm C and D). Because of logistic reasons, the trial started with the sunitinib (arm A and B) cohorts and bevacizumab (Arms C and D) cohorts were recruited after completion of Arms A and B. All patients received cisplatin (75 mg/m^2 on day 1) and gemcitabine (1 g/m^2 on days 1 and 8) every 3 weeks. Patients were randomly assigned 1:1 to oral sunitinib 12.5 mg (arm A) or 25 mg (arm B) daily for 1 week, starting 1 week before each cycle of cisplatin and gemcitabine. Arm C and arm D patients received bevacizumab 7.5 mg/kg and 2.5 mg/kg, respectively, given every 3 weeks, starting 1 week prior to each cycle of the same chemotherapy. Patients with stages III–IVB NPC received three cycles of the study treatment as induction chemotherapy prior to concurrent chemo-radiotherapy. Patients with metastatic NPC received up to six cycles of the treatment until disease progression or intolerable toxic effects.

Prespecified treatment dose modifications were allowed after the occurrence and resolution of predefined grade 3–4 hematologic or grade 2–4 nonhematologic toxic effects. Radiotherapy employed simultaneous boost intensity-modulated technique (IMRT; Supplementary Methods).

Assessment

Baseline tumor assessments were performed within 4 weeks before the start of treatment. ^{18}FDG-PET-CT scan was repeated at end of three cycles of induction chemotherapy for patients with stage III–IVB, after the third and last cycle of systemic treatment for patients with metastatic NPC; and the best metabolic responses for each patient were analyzed. ^{18}FDG-PET-CT scan was performed using a standard protocol (Supplementary Methods). The sum of SUVmax of the primary nasopharyngeal lesion and lymph nodes and any distant metastatic sites for each scan was compared between the baseline and the postinduction chemotherapy scans. Complete metabolic response (mCR) was defined by the resolution of all metabolically active sites to background levels of the relevant surrounding tissue. Plasma sampling for Epstein–Barr virus (EBV) DNA to evaluate tumor burden and soluble VEGF were collected at baseline, after 1 week of sunitinib/bevacizumab, on cycle 2 day 1, on cycle 3 day 1, and 28 days postinduction therapy [end of induction therapy treatment (EOT)]. Plasma EBV DNA was based on quantification of *Bam*HI-W DNA fragments via an amplicon-based next-generation sequencing method at Lucence Diagnostics (14). VEGF-A was analyzed using dual oligonucleotide-tagged antibody binding and quantitative PCR (Olink Proteomics, https://www.olink.com). All patients who received at least one dose of chemotherapy were evaluated for toxicity every cycle and adverse events were graded according to the NCI Common Terminology Criteria for Adverse Events, version 4.0.

The primary endpoint of the study was objective tumor response (metabolic response and RECIST 1.1) to induction chemotherapy. Secondary endpoints include tolerability to study treatment as graded by the percentage of patients experiencing toxicities, toxicities leading to dose delays or discontinuation, tumor response after definitive concurrent chemotherapy and radiotherapy, and relapse-free survival (RFS) in radiotherapy-treated locally advanced NPC. RFS is defined as

the time from assignment to disease progression or death from any cause, whichever occurred first. Nasopharyngeal biopsies were taken at baseline and 7 days after initiating the first cycle of sunitinib or bevacizumab and IHC studies were performed by two research pathologists blinded to the clinical data. The effect of VEGF inhibition on tumor microvasculature was measured using IHC and comparing the endothelial cells and pericyte coverage and expressing changes in microvessel densities. Changes in immune infiltration into the tumor microenvironment were determined by scoring for inflammatory and immune infiltrates (Supplementary Methods).

Statistical analyses

A primary endpoint of the study for sample size calculation was mCR to induction chemotherapy. This was estimated to be around 5% for the worst study arm and 30% for the best study arm. Sample size calculation utilized the randomized phase II design based on statistical selection theory. With four study arms, 19 patients per study arm would yield the probability of 0.91 of selecting the schedule that has a true mCR rate of 30%. Time-to-event outcomes were estimated using the Kaplan–Meier method. Comparisons of metabolic responses between the four arms were done first using Fisher exact test of independence. For correlative tissue analysis, one-tailed Wilcoxon signed rank was used to establish the significance of any changes observed. All statistical analyses were performed using either IBM SPSS statistics version 25 or GraphPad Prism version 6.

Results

Patient characteristics

Between May 2012 and January 2019, 77 patients were enrolled in the study; 15 to arm A, 18 to arm B, 20 to arm C, and 24 to arm D. One patient in arm C was ineligible and excluded from analyses because he developed new cardiac arrhythmia prior to study initiation (**Fig. 1**).

Patient and disease characteristics at baseline were similar between treatment groups (**Table 1**). Twenty-nine patients (37%) had preexisting arterial hypertension and 7 patients (9%) had coronary artery disease.

Treatment compliance

Among 61 patients with locally advanced (stage III–IVB) NPC (**Table 1**), 55 patients (83.3%) received all three cycles of induction chemotherapy: 11 (100%) in arm A, 15 (100%) in arm B, 15 (93.8%) in arm C, and 14 (73.7%) in arm D. Discontinuation of chemotherapy was mostly due to toxicities ($n = 6$; two in arm B, one in arm C, and three in arm D) and patients' withdrawal of consent midway of the study ($n = 5$; one in arm C and four in arm D). One patient with metastatic NPC each in arm B and D did not receive the intended six cycles of chemotherapy due to disease progression. Dose modification due to adverse events occurred in 3 (20%) patients in arm A, 4 (22%) in arm B, 3 (16%) in arm C, and 3 (13%) in arm D, and treatment dose was delayed in 7 (47%) patients in arm A, 9 (50%) in arm B, 11 (58%) in arm C, and 14 (58%) in arm D (**Fig. 1**).

Treatment safety

Myelosuppression was the commonest toxicity with a higher incidence of leukopaenia (84.8% vs. 55.8%, $P = 0.007$) and thrombocytopaenia (90.9% vs. 18.6%, $P < 0.001$) in the arms containing sunitinib than those receiving bevacizumab (**Table 2**). Notably, no patient had clinically significant tumoral bleeding and all serial biopsies following antiangiogenic therapy were uneventful. There was no treatment-related death.

Tumor response

A comparison of mCR rates showed significant differences between the four arms ($P = 0.001$). Furthermore, pairwise

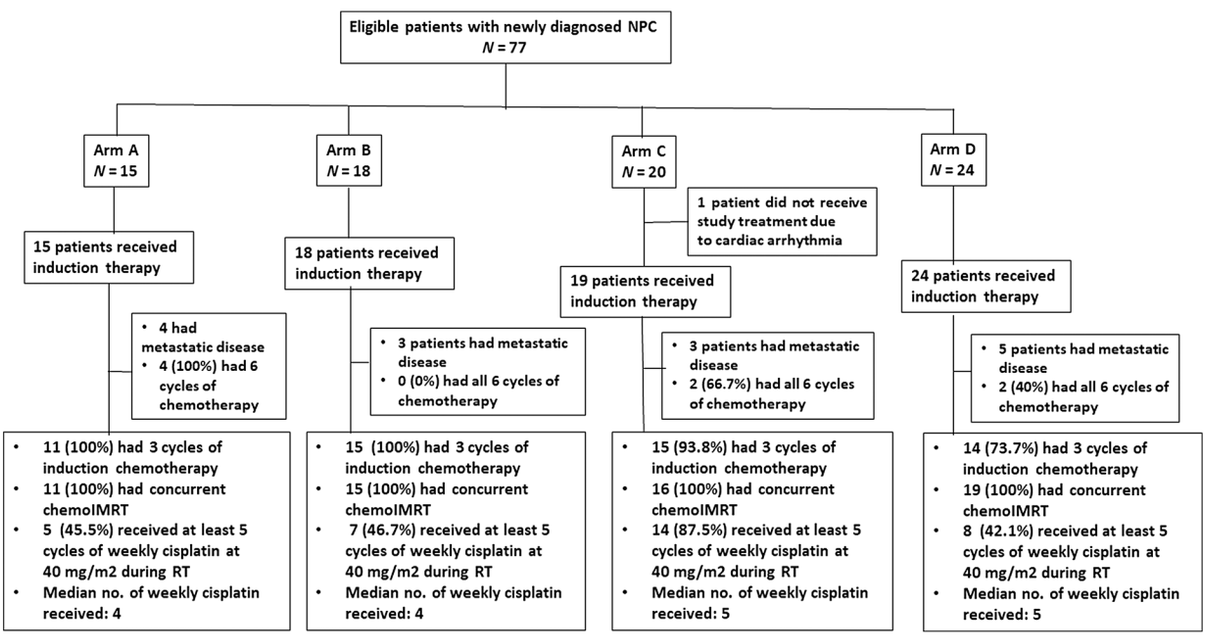

Figure 1.
CONSORT diagram.

Table 1. Patient characteristics.

	Arm A (sunitinib 12.5 mg), $n = 15$	Arm B (sunitinib 25 mg), $n = 18$	Arm C (bevacizumab 7.5 mg/kg), $n = 19$	Arm D (bevacizumab 2.5 mg/kg), $n = 24$
Median age (range): years	51 (36–61)	56.5 (42–74)	60 (32–68)	56.5 (35–80)
Sex: No. (%)				
Male	11 (73%)	17 (94%)	18 (95%)	15 (63%)
Female	4 (27%)	1 (6%)	1 (5%)	9 (37%)
ECOG: No. (%)				
0	7 (47%)	16 (89%)	13 (68%)	19 (79%)
1	8 (53%)	2 (11%)	6 (32%)	5 (21%)
Race: No. (%)				
Chinese	13 (87%)	13 (72%)	13 (68%)	22 (92%)
Malay	2 (13%)	4 (22%)	3 (16%)	1 (4%)
Other	0	1 (6%)	3 (16%)	1 (4%)
Tumor size: No. (%)				
T1	1 (7%)	5 (28%)	1 (5%)	4 (17%)
T2	0	0	2 (11%)	0
T3	2 (13%)	1 (5%)	2 (11%)	2 (8%)
T4	12 (80%)	12 (67%)	14 (74%)	18 (75%)
Nodal status: No. (%)				
N0	0	0	1 (5%)	1 (4%)
N1	3 (20%)	6 (33%)	7 (37%)	7 (29%)
N2	8 (53%)	5 (28%)	6 (32%)	8 (33%)
N3	4 (27%)	7 (39%)	5 (26%)	8 (33%)
TNM stage: No. (%)				
III	0	0	1 (5%)	0
IVA	7 (47%)	10 (56%)	12 (63%)	14 (58%)
IVB	4 (27%)	5 (28%)	3 (16%)	5 (21%)
IVC (metastatic)	4 (27%)	3 (17%)	3 (16%)	5 (21%)

comparisons with Bonferroni correction ($P < 0.0083$ considered significant) showed superior response rates in arm C (42% mCR) compared with arm A (0%, $P = 0.001$) and arm B (5.6%, $P = 0.008$) but similar to arm D (12.5%, $P = 0.017$) (**Tables 3A** and **3B**). The waterfall plots of metabolic responses and tumor responses in the four study arms, respectively, are shown in **Fig. 2A** and **B**. An example of mCR from induction therapy of a patient in arm C is shown in Supplementary Fig. S2.

RFS for patients with locally advanced disease

Sixty-one patients (11 patients in arm A, 15 in arm B, 16 in arm C, and 19 in arm D) had locally advanced disease and received chemoradiation with curative intent, and were followed up for RFS. The median follow-up for patients in arms A and B was 53.2 months and for arms C and D was 22.4 months.

Overall, 20 of 61 patients (32.8%) with stage III–IVB NPC had disease progression. The 3-year RFS rates were 64% [confidence

Table 2. Treatment toxicity.

	Arm A (sunitinib 12.5 mg), $n = 15$		Arm B (sunitinib 25 mg), $n = 18$		Arm C (bevacizumab 7.5 mg/kg), $n = 19$		Arm D (bevacizumab 2.5 mg/kg), $n = 24$	
Toxicity	**Grade 1 or 2 No. (%)**	**Grade 3 or 4 No. (%)**	**Grade 1 or 2 No. (%)**	**Grade 3 or 4 No. (%)**	**Grade 1 or 2 No. (%)**	**Grade 3 or 4 No. %)**	**Grade 1 or 2 No. (%)**	**Grade 3 or 4 No. (%)**
Any	3 (20)	12 (80)	4 (22.2)	14 (77.8)	11 (57.9)	7 (36.8)	10 (41.7)	13 (54.2)
Anemia	6 (40.0)	0	3 (16.7)	0	7 (36.8)	0	2 (8.3)	2 (8.3)
Thrombocytopaenia	8 (53.3)	6 (40.0)	9 (50)	7 (38.9)	6 (31.6)	0	1 (4.2)	1 (4.2)
Leucopenia	3 (20)	10 (66.7)	3 (16.7)	12 (66.7)	5 (26.3)	6 (31.6)	6 (25)	7 (29.2)
Febrile neutropenia	0	0	0	0	0	0	1 (4.2)	1 (4.2)
Emesis	1 (6.7)	1 (6.7)	1 (5.6)	2 (11.1)	0	0	3 (12.5)	1 (4.2)
Diarrhea	0	0	2 (11.1)	0	0	0	3 (12.5)	0
Hyponatremia	1 (6.7)	1 (6.7)	4 (22.2)	3 (16.7)	2 (10.5)	0	4 (16.7)	2 (8.3)
Elevated creatinine	0	0	0	0	2 (10.5)	0	0	1 (4.2)
Peripheral neuropathy	1 (6.7)	0	0	0	1 (5.3)	0	5 (20.8)	0
Hypertension	4 (26.7)	2 (13.3)	9 (50)	2 (11.1)	11 (57.9)	1 (5.3)	12 (50)	4 (16.7)
Proteinuria	0	0	0	0	0	0	0	1 (4.2)
Vascular event[a]	0	0	0	1 (5.6)	1 (5.3)	0	0	0

[a]Vascular event includes a grade 2 stroke and grade 4 cardiac arrest.

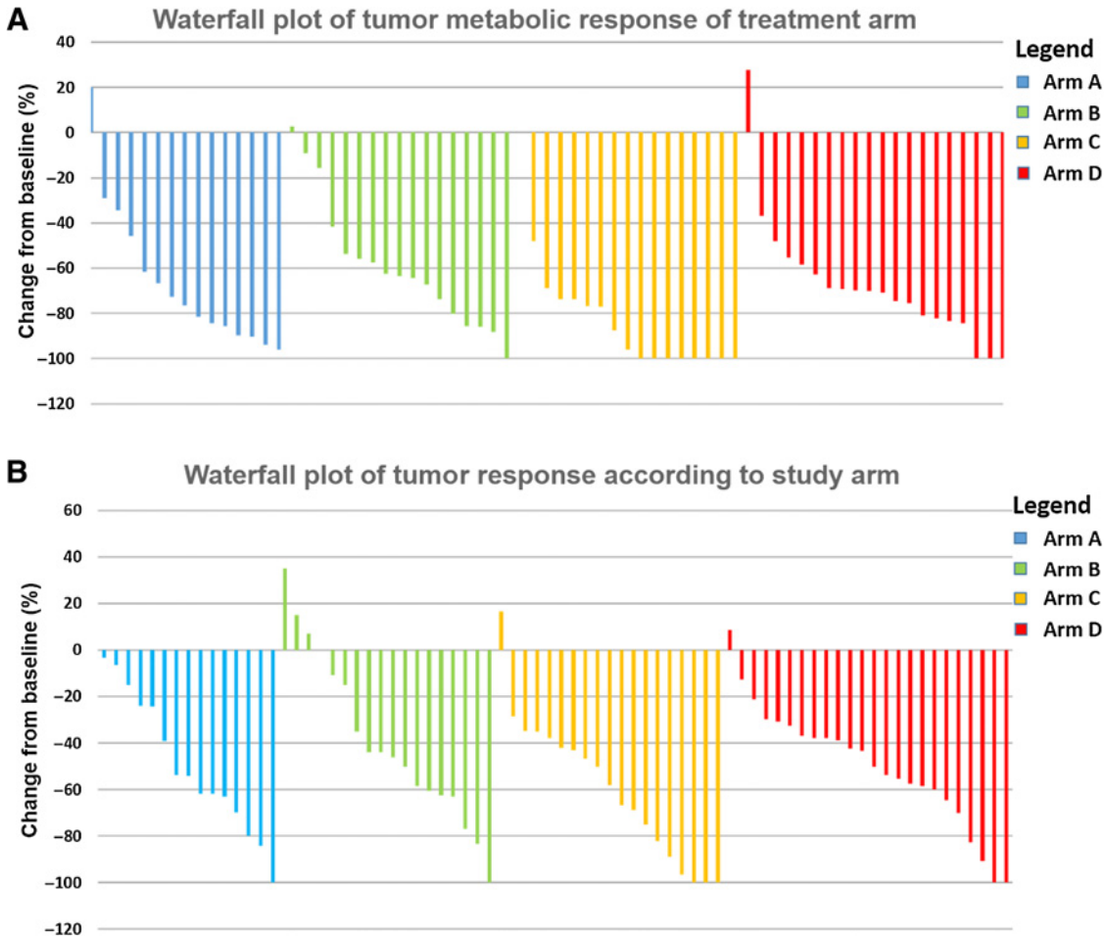

Figure 2.

Waterfall plots by study arms of patients showing tumor metabolic response (**A**) and tumor response to the combination treatment (**B**). The *y*-axes show the percentage change in sum of SUVmax and RECIST measurements after treatment, respectively. The *x*-axes represent the patient numbers.

interval (CI), 36–92], 60% (CI, 35–86), and 88% (CI, 72–104) for arms A, B, and C, respectively (Supplementary Fig. S3). The 2-year locoregional failure occurred in 3 (27.3%) patients in arm A, 2 (13.3%) in arm B, 2 (12.5%) in arm C, and 2 (10.5%) in arm D, respectively. The 2-year distant failure occurred in 2 (18.2%) patients in arm A, 4 (26.7%) in arm B, 2 (12.5%) in arm C, and 3 (15.7%) in arm D, respectively.

To validate the clinical utility of metabolic response, RFS of patients treated with chemoradiation was analyzed according to the depth of metabolic response (80% or more vs. less than 80%). Data showed a higher RFS for the better responders who underwent chemoIMRT: 5-year PFS was 80.2% versus 42.2%; log-rank test $P = 0.016$ (Supplementary Fig. S4). Comparison of the depth of metabolic response showed that 47% patients in arm A, 28% in arm B, 62.5% in arm C, and 33% in arm D experienced 80% or more reduction in the sum of SUVmax in lesions.

Plasma EBV DNA titres and circulating VEGF-A with induction therapy

A total of 59 plasma samples were analyzed for baseline EBV DNA levels: the mean and SD were 14,480 ± 28,383 IU/mL in arm A, 6,518 ± 16,157 IU/mL in arm B, 13,615 ± 27,722 IU/mL in arm C, and 5,883 ± 10,382 IU/mL in arm D. A total of 57 patients had plasma EBV DNA viral load remeasured at day 1 of cycle 3 the mean and SD were 560 ± 1,569 IU/mL in arm A, 229 ± 315 IU/mL in arm B, 65 ± 135 IU/mL in arm C, and 1,115 ± 3,416 IU/mL in arm D. It reached undetectable levels (defined as less than 50 IU/mL of EBV DNA) in 7/12 (58.3%), 3/14 (21.4%), 13/18 (72.2%), and 8/13 (61.5%) of patients in arms A, B, C, and D, respectively (Supplementary Fig. S5A).

A total of 9/11 in arm A, 14/14 in arm B, 18/18 in arm C, and 15/15 in arm D showed above normal circulating VEGF levels in their baseline samples. In patients receiving sunitinib (arms A and B), the VEGF levels remained high at the beginning of cycle 1 (C1D1) and in 4/8 (50%) of patients of arm A and 6/9 (66%) of arm B at EOT. In contrast, in patients receiving 7.5 mg/kg of bevacizumab (arm C), circulating VEGF levels in 17/18 (94%) of the cohort fell to within normal limits within 7 days of bevacizumab treatment (C1D1) and 15/15 (100%) remained within normal limits at EOT (Supplementary Fig. S5B).

Maturation of tumor microvasculature and changes in the microenvironment

Enumeration of mature pericyte covered microvasculature showed increase in mature vessels post anti-VEGF treatment in arms A and C

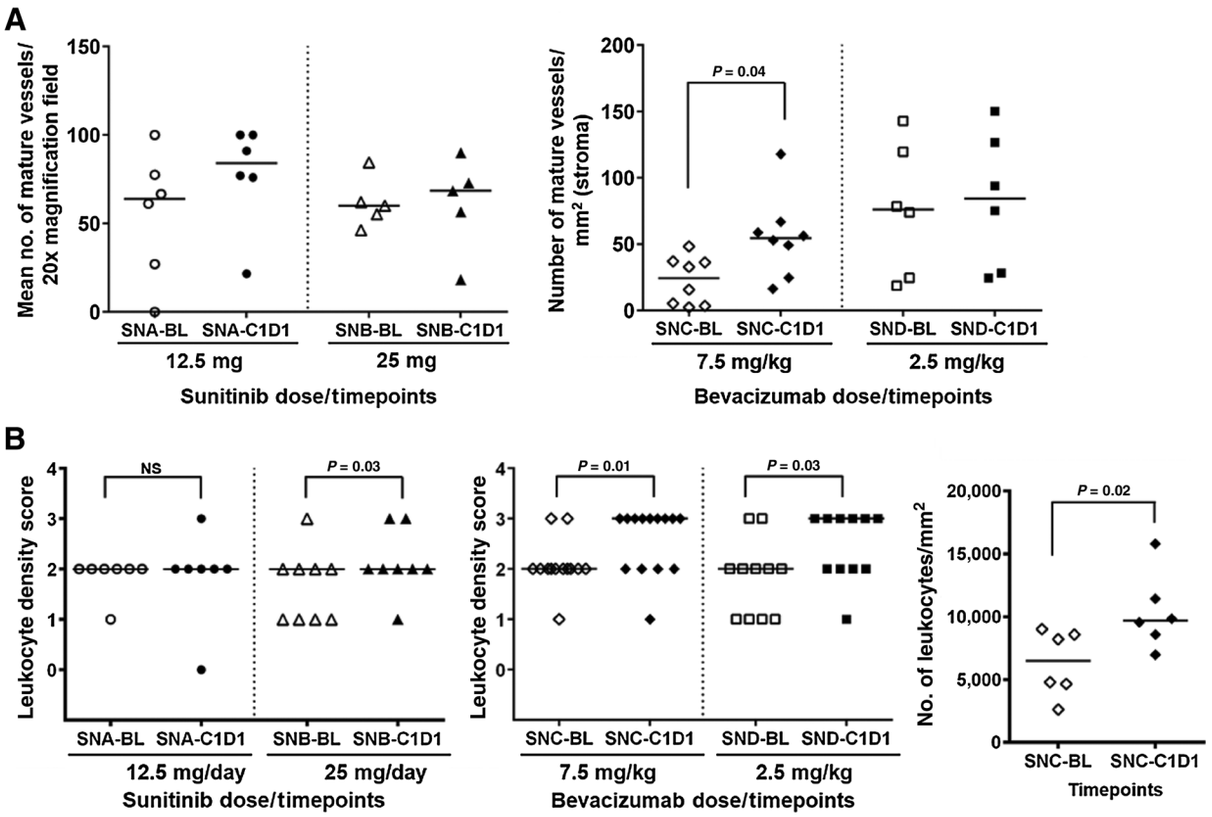

Figure 3.

Bevacizumab at 7.5 mg/kg dose is more effective than sunitinib in inducing blood vessel maturation and in the recruitment of immune cells into the NPC primary lesion. **A,** The mean number of $SMA^+/CD34^+$ vessels/20× magnification field in baseline (BL) and 7 days after start of sunitinib treatment (C1D1) samples of arms A and B (left). Number of $SMA^+/CD31^+$ vessels/mm^2 in BL and 7 days after start of bevacizumab treatment (C1D1) samples of arms C and D (right). **B,** Cellular infiltrate scores for BL and C1D1 samples of patients treated with sunitinib (arms A and B), and with bevacizumab (arms C and D), respectively (left and middle). Leukocyte density in BL and C1D1 tissue samples from 6 representative arm C patients as determined by Image J (right).

(**Fig. 3A**; Supplementary Fig. S6A) without change in microvessel density with all four arms (Supplementary Fig. S6B).

Morphologic examination of the hematoxylin and eosin sections suggested an increase in immune and inflammatory cell infiltrate into the primary lesion in response to 7.5 mg/kg of bevacizumab treatment (**Fig. 3B**; Supplementary Fig. S7) prior to start of chemotherapy, indicating better chemotaxis and trafficking of immune cells into the tumor microenvironment. The predominant cellular infiltrate were lymphocytes comprising CD4 helper and CD8 cytotoxic T cells. Macrophages, neutrophils, and sometimes eosinophils were also present albeit in much lower numbers compared with the lymphocytic cells. To confirm this observation, the number of leukocytes in representative arm C samples ($n = 6$) were quantified using Image J (NIH) Software with the Colour Deconvolution Plugin. The median leukocyte density and range for the baseline and C1D1 samples were 6,501 cells/mm^2 (range: 2,622–8,999 cells/mm^2) and 9,695 cells/mm^2 (range: 6,976–15,796 cells/mm^2), respectively (**Fig. 3B**).

Discussion

VEGF is highly expressed in NPC through oncogenic EBV latent membrane protein 1 (15), and expression correlates with metastases and prognosis (16), inspiring much interest in developing anti-VEGF therapy for NPC. Previous phase II studies in recurrent/metastatic NPC with anti-VEGF multikinase inhibitors yielded modest activity, with added risk of catastrophic hemorrhage from previously irradiated head and neck region (17, 18). As first-line therapy, bevacizumab combined with standard cisplatin-based chemoradiation was shown to be tolerable and achieved favorable disease control in RTOG 0615 study, raising the potential of incorporating antiangiogenic therapy with chemotherapy (19). Our study supports the concept of normalization of microvasculature with antiangiogenic therapy, which may improve chemotherapy delivery and immune infiltration that is associated with favorable prognosis (20). The antiangiogenic dosage used in all arms of the study did not result in excess of tumor hemorrhage, allowed serial biopsies to be done safely, and did not compromise definitive chemoradiation.

Among the four study arms with two different doses of sunitinib and bevacizumab, the arm with bevacizumab at 7.5 mg/kg was superior in tolerability, antitumor, plasma EBV, and VEGF responses to induction therapy. The 3-year RFS of 88% for predominantly stage IVA/B patients with locally advanced disease in this arm compares favorably with concurrent chemoradiation, where the 3-year RFS was ranged from 66% to 73% (21–25).

Induction chemotherapy is known to have a profound effect on NPC and the response rates in all four arms of our study were above 80%, which is consistent with effectiveness of the cisplatin and gemcitabine combination. Previously, investigators have shown that

Table 3A. Response to induction treatment.

Response	Arm A (sunitinib 12.5 mg), $n = 15$		Arm B (sunitinib 25 mg), $N = 18$		Arm C (bevacizumab 7.5 mg/kg), $n = 19$		Arm D (bevacizumab 2.5 mg/kg), $n = 24$	
	CT/MRI	PET	CT/MRI	PET	CT/MRI	PET	CT/MRT	PET
Complete No. (%)	0	0	1 (5.6)	1 (5.6)	3 (15.8)	8 (42.1)	2 (8.3)	3 (12.5)
Partial No. (%)	13 (86.7)	13 (86.7)	14 (77.8)	13 (72.2)	14 (73.7)	9 (47.4)	18 (75)	16 (66.7)
Overall %	86.7	86.7	83.4	77.8	89.5	89.5	83.3	79.2
Stable No. (%)	2 (13.3)	2 (13.3)	1 (5.6)	2 (11.1)	2 (10.5)	0 0	4 (16.7)	1 (4.2)
Progression No. (%)	0	0	1 (5.6)	1 (5.6)	0	0	0	0
Not assessable[a] No. (%)	0	0	1 (5.6)	1 (5.6)	0	2 (10.5)	0	4 (16.7)

[a]Response to induction treatment was not assessable as patients did not undergo interval CT/MRI/PET scans.

Table 3B. Response to induction chemotherapy followed by concurrent chemoradiotherapy treatment.

Responses	Arm A (sunitinib 12.5 mg), $n = 11$	Arm B (sunitinib 25 mg), $n = 15$	Arm C (bevacizumab 7.5 mg/kg), $n = 16$	Arm D (bevacizumab 2.5 mg/kg), $n = 19$
Complete No. (%)	9 (81.8)	11 (73.3)	14 (87.5)	15 (78.9)
Partial No. (%)	2 (18.2)	3 (20)	2 (12.5)	4 (21.1)
Overall (%)	100	93.3	100	100
Not assessable No. (%)	0	1 (6.7)	0	0

PET CT scan after induction chemotherapy may be a good early indicator of clinical outcome as metabolic responses observed during induction chemotherapy precedes anatomic responses on MRI (13, 26). Our study validated this in patients with locally advanced disease, where RFS was significantly prolonged for patients with 80% or better reduction in sum of SUV_{max} for the primary and neck lymph nodes. mCR rates were highest in the 7.5 mg/kg bevacizumab arm and translated to favorable RFS in this study arm. It should be noted that there are no current guidelines for defining mCR in NPC, and our criteria was consistent with both EORTC and PERCIST guidelines (27).

The favorable clinical outcome of arm C is supported by observed effects in both plasma biomarkers and tumor microenvironment. Arm C had the greatest suppression of both plasma EBV DNA titre and VEGF levels by the second cycle of treatment. Of note, patients with detectable plasma EBV postinduction chemotherapy and higher VEGF levels have worse prognosis in NPC (28). The IHC studies supported the hypothesis that anti-VEGF therapy promotes microvasculature maturation and enhanced immune infiltration within a week, with bevacizumab 7.5 mg/kg demonstrating both effects. Anti-VEGF treatment has been proposed to improve immune cell trafficking and alleviate hypoxia to activate immune function in tumors, and survival in NPC is associated with abundance of tumor lymphocytic infiltration (20). Though the optimal dose and duration of normalization of vasculature, following anti-VEGF treatment is uncertain, the sunitinib-containing regimen is unlikely to be tolerable at higher doses due to off target effects that cause myelosuppression (29).

Addition of bevacizumab to cisplatin/gemcitabine in metastatic disease potentially adds therapeutic benefit, but the issue of hemorrhagic events needs to be evaluated in the context of prior chemoradiation. The combination of antiangiogenic therapy with PD-1/PDL-1 inhibitors has shown promising tumor responses in cancers such as non–small lung cancers and renal cell cancers (30). The positive effects of antiangiogenic therapy on tumor perfusion and immune cell trafficking into the nasopharyngeal cancer seen in our study encourage new studies combining immunotherapy and antiangiogenic therapy in metastatic nasopharyngeal cancers. For locally advanced NPC, this study together with the data from RTOG 0615 support the need for further studies to establish the role of bevacizumab in the induction chemotherapy and concurrent chemoradiotherapy phases of treatment.

Disclosure of Potential Conflicts of Interest

W.-Q. Chong reports nonfinancial support from MSD (conference support) and Amgen (conference support) outside the submitted work. R. Sundar reports other from BMS (honararia for talks/advisory board), Merck (honararia for talks/advisory board), Eisai (honararia for talks/advisory board), Bayer (honararia for talks/advisory board), Taiho (honararia for talks/advisory board), MSD (honararia for talks/advisory board), Eli Lilly (honararia for talks/advisory board), Roche (honararia for talks/advisory board), and Astra Zeneca (honararia for talks/advisory board) and grants from MSD and Paxman Coolers outside the submitted work. A. Jeyasekharan reports grants and personal fees from Janssen and personal fees from AstraZeneca and MSD outside the submitted work. S.-C. Lee reports grants and other from Pfizer (research grant for investigator-initiated studies; honorarium for advisory boards and as invited speaker at conferences), Eisai (research grant for investigator-initiated studies; honorarium for advisory boards and invited speaker at conferences), and Taiho (research grant for investigator-initiated studies) and other from Amgen (travel support to conference), Novartis (honorarium for advisory boards and invited speaker at conferences), Astra Zeneca (honorarium for advisory boards and invited speaker at conferences), Roche (honorarium for advisory boards and invited speaker at conferences), ACT Genomics (honorarium for advisory boards and invited speaker at conferences), MSD (honorarium for advisory board), and Eli Lilly (honorarium for advisory board) outside the submitted work. B.-C. Tai reports other from Boehringer Ingelheim Singapore Pte Ltd (conduct workshop), Boehringer Ingelheim (Malaysia) Sdn Bhd (conduct workshop), and Wiley-Blackwell (royalty) outside the submitted work. B.-C.Goh reports grants from National Medical Research Council, Singapore during the conduct of the study. No potential conflicts of interest were disclosed by the other authors.

Authors' Contributions

W.Q. Chong: Data curation, formal analysis, investigation, writing-original draft, writing-review and editing. **C.M. Lim:** Investigation. **A.K. Sinha:** Investigation, methodology. **C.S. Tan:** Data curation, investigation, methodology, project administration. **G.H.J. Chan:** Investigation. **Y. Huang:** Investigation. **N. Barr Kumarakulasinghe:** Investigation. **R. Sundar:** Investigation. **A.D. Jeyasekharan:** Investigation. **W.-S. Loh:** Investigation. **J.K. Tay:** Investigation. **K. Yadav:** Investigation. **L. Wang:** Investigation, methodology, project administration. **A.L. Wong:** Investigation, methodology, project administration. **L.R. Kong:** Investigation. **R.A. Soo:** Investigation, writing-review and editing. **J.A. Lau:** Investigation. **Y.Y. Soon:** Formal analysis, investigation. **R.M. Goh:** Data curation. **F.C.H. Ho:** Investigation. **S.M. Chong:** Formal analysis, investigation, methodology. **S.-C. Lee:** Conceptualization, investigation. **K.S. Loh:** Investigation. **B.C. Tai:** Formal analysis, methodology. **Y.C. Lim:** Formal analysis, investigation, methodology, writing-original draft, project administration, writing-review and editing. **B.C. Goh:** Conceptualization, resources, data curation, formal analysis, supervision, funding acquisition, validation, investigation, methodology, writing-original draft, project administration, writing-review and editing.

Acknowledgments

This study is supported by Clinical Scientist Award awarded by National Medical Research Council of Singapore to B.-C. Goh (NMRC/CSA-SI/0006/2016 and NMRC/CG/012/2013).

We like to thank all the patients and their families who participated in this trial. We also wish to express our gratitude and respect to our collaborator and colleague, the late S.-M. Chong for his contributions including development of methodology and analysis of data in the project. S.-M. Chong passed away in August 2019.

The costs of publication of this article were defrayed in part by the payment of page charges. This article must therefore be hereby marked *advertisement* in accordance with 18 U.S.C. Section 1734 solely to indicate this fact.

Received May 8, 2020; revised June 26, 2020; accepted August 4, 2020; published first August 14, 2020.

References

1. Chan KCA, Woo JKS, King A, Zee BCY, Lam WKJ, Chan SL, et al. Analysis of plasma Epstein-Barr virus DNA to screen for nasopharyngeal cancer. N Engl J Med 2017;377:513–22.
2. Lee AW, Ma BB, Ng WT, Chan AT. Management of nasopharyngeal carcinoma: current practice and future perspective. J Clin Oncol 2015;33:3356–64.
3. Sham JS, Choy D, Choi PH. Nasopharyngeal carcinoma: the significance of neck node involvement in relation to the pattern of distant failure. Br J Radiol 1990;63:108–13.
4. Kang M, Zhou P, Li G, Yan H, Feng G, Liu M, et al. Validation of the 8th edition of the UICC/AJCC staging system for nasopharyngeal carcinoma treated with intensity-modulated radiotherapy. Oncotarget 2017;8:70586–94.
5. Sun Y, Li WF, Chen NY, Zhang N, Hu GQ, Xie FY, et al. Induction chemotherapy plus concurrent chemoradiotherapy versus concurrent chemoradiotherapy alone in locoregionally advanced nasopharyngeal carcinoma: a phase 3, multicentre, randomised controlled trial. Lancet Oncol 2016;17:1509–20.
6. Zhang Y, Chen L, Hu GQ, Zhang N, Zhu XD, Yang KY, et al. Gemcitabine and cisplatin induction chemotherapy in nasopharyngeal carcinoma. N Engl J Med 2019;381:1124–35.
7. Zhang B, Li MM, Chen WH, Zhao JF, Chen WQ, Dong YH, et al. Association of chemoradiotherapy regimens and survival among patients with nasopharyngeal carcinoma: a systematic review and meta-analysis. JAMA Netw Open 2019;2:e1913619.
8. Goel S, Duda DG, Xu L, Munn LL, Boucher Y, Fukumura D, et al. Normalization of the vasculature for treatment of cancer and other diseases. Physiol Rev 2011;91:1071–121.
9. Jain RK. Normalization of tumor vasculature: an emerging concept in antiangiogenic therapy. Science 2005;307:58–62.
10. Fukumura D, Kloepper J, Amoozgar Z, Duda DG, Jain RK. Enhancing cancer immunotherapy using antiangiogenics: opportunities and challenges. Nat Rev Clin Oncol 2018;15:325–40.
11. Wang F, Peng L, Wang Y, Liu X. A meta-analysis of vascular endothelial growth factor for nasopharyngeal cancer prognosis. Front Oncol 2018;8:486.
12. Kamoun WS, Ley CD, Farrar CT, Duyverman AM, Lahdenranta J, Lacorre DA, et al. Edema control by cediranib, a vascular endothelial growth factor receptor-targeted kinase inhibitor, prolongs survival despite persistent brain tumor growth in mice. J Clin Oncol 2009;27:2542–52.
13. Yen RF, Chen TH, Ting LL, Tzen KY, Pan MH, Hong RL. Early restaging whole-body (18)F-FDG PET during induction chemotherapy predicts clinical outcome in patients with locoregionally advanced nasopharyngeal carcinoma. Eur J Nucl Med Mol Imaging 2005;32:1152–9.
14. Vo JH, Nei WL, Hu M, Phyo WM, Wang F, Fong KW, et al. Comparison of circulating tumour cells and circulating cell-free Epstein-Barr virus DNA in patients with nasopharyngeal carcinoma undergoing radiotherapy. Sci Rep 2016;6:13.
15. Murono S, Inoue H, Tanabe T, Joab I, Yoshizaki T, Furukawa M, et al. Induction of cyclooxygenase-2 by Epstein-Barr virus latent membrane protein 1 is involved in vascular endothelial growth factor production in nasopharyngeal carcinoma cells. Proc Natl Acad Sci U S A 2001;98:6905–10.
16. Guang-Wu H, Sunagawa M, Jie-En L, Shimada S, Gang Z, Tokeshi Y, et al. The relationship between microvessel density, the expression of vascular endothelial growth factor (VEGF), and the extension of nasopharyngeal carcinoma. Laryngoscope 2000;110:2066–9.
17. Hui EP, Ma BB, King AD, Mo F, Chan SL, Kam MK, et al. Hemorrhagic complications in a phase II study of sunitinib in patients of nasopharyngeal carcinoma who has previously received high-dose radiation. Ann Oncol 2011;22:1280–7.
18. Lim WT, Ng QS, Ivy P, Leong SS, Singh O, Chowbay B, et al. A Phase II study of pazopanib in Asian patients with recurrent/metastatic nasopharyngeal carcinoma. Clin Cancer Res 2011;17:5481–9.
19. Lee NY, Zhang Q, Pfister DG, Kim J, Garden AS, Mechalakos J, et al. Addition of bevacizumab to standard chemoradiation for locoregionally advanced nasopharyngeal carcinoma (RTOG 0615): a phase 2 multi-institutional trial. Lancet Oncol 2012;13:172–80.
20. Wang YQ, Chen YP, Zhang Y, Jiang W, Liu N, Yun JP, et al. Prognostic significance of tumor-infiltrating lymphocytes in nondisseminated nasopharyngeal carcinoma: a large-scale cohort study. Int J Cancer 2018;142:2558–66.
21. Al-Sarraf M, LeBlanc M, Giri PG, Fu KK, Cooper J, Vuong T, et al. Chemoradiotherapy versus radiotherapy in patients with advanced nasopharyngeal cancer: phase III randomized Intergroup study 0099. J Clin Oncol 1998;16:1310–7.
22. Chan AT, Teo PM, Ngan RK, Leung TW, Lau WH, Zee B, et al. Concurrent chemotherapy-radiotherapy compared with radiotherapy alone in locoregionally advanced nasopharyngeal carcinoma: progression-free survival analysis of a phase III randomized trial. J Clin Oncol 2002;20:2038–44.
23. Lee AW, Lau WH, Tung SY, Chua DT, Chappell R, Xu L, et al. Preliminary results of a randomized study on therapeutic gain by concurrent chemotherapy for regionally-advanced nasopharyngeal carcinoma: NPC-9901 Trial by the Hong Kong Nasopharyngeal Cancer Study Group. J Clin Oncol 2005;23:6966–75.
24. Wee J, Tan EH, Tai BC, Wong HB, Leong SS, Tan T, et al. Randomized trial of radiotherapy versus concurrent chemoradiotherapy followed by adjuvant chemotherapy in patients with American Joint Committee on Cancer/International Union against cancer stage III and IV nasopharyngeal cancer of the endemic variety. J Clin Oncol 2005;23:6730–8.
25. Lee AW, Tung SY, Chan AT, Chappell R, Fu YT, Lu TX, et al. Preliminary results of a randomized study (NPC-9902 Trial) on therapeutic gain by concurrent chemotherapy and/or accelerated fractionation for locally advanced nasopharyngeal carcinoma. Int J Radiat Oncol Biol Phys 2006;66:142–51.
26. Wong KH, Panek R, Welsh L, McQuaid D, Dunlop A, Riddell A, et al. The predictive value of early assessment after 1 cycle of induction chemotherapy with 18F-FDG PET/CT and diffusion-weighted MRI for response to radical chemoradiotherapy in head and neck squamous cell carcinoma. J Nucl Med 2016;57:1843–50.

27. O JH, Lodge MA, Wahl RL. Practical PERCIST: a simplified guide to PET response criteria in solid tumors 1.0. Radiology 2016;280:576–84.
28. Huang CL, Sun ZQ, Guo R, Liu X, Mao YP, Peng H, et al. Plasma Epstein-Barr virus DNA load after induction chemotherapy predicts outcome in locoregionally advanced nasopharyngeal carcinoma. Int J Radiat Oncol Biol Phys 2019;104:355–61.
29. Kumar R, Crouthamel MC, Rominger DH, Gontarek RR, Tummino PJ, Levin RA, et al. Myelosuppression and kinase selectivity of multikinase angiogenesis inhibitors. Br J Cancer 2009;101:1717–23.
30. Xin Yu J, Hodge JP, Oliva C, Neftelinov ST, Hubbard-Lucey VM, Tang J. Trends in clinical development for PD-1/PD-L1 inhibitors. Nat Rev Drug Discov 2020;19:163–4.